

GRAIN BOUNDARY WETTING IN THE W-Ni SYSTEM

V.Glebovsky¹, B.Straumal^{1,2}, V.Semenov¹, V.Sursaeva¹, W.Gust²

¹Institute of Solid State Physics, Russian Academy of Sciences,
Chernogolovka, Moscow District, 142432 Russia

²Max-Planck-Institut für Metallforschung, Seestr. 75,
D-7000 Stuttgart 1, Germany

ZUSAMMENFASSUNG:

Es wurde das Eindringen von Ni entlang der Korngrenzen (KG) in W-Vielkristallen bei verschiedenen Temperaturen (1600, 1800 und 2000°C) oberhalb der eutektischen Temperatur des Systems W-Ni untersucht. Bei 1600°C wurden drei verschiedene Gruppen von KG beobachtet: a) KG, die von Ni-reicher Schmelze benetzt sind; b) KG, die von Ni-reicher Schmelze teilweise benetzt sind; c) KG, die von Ni-reicher Schmelze nicht benetzt sind. Das bedeutet, daß man den KG-Benetzungphasenübergang im W-Ni-System beobachten kann. Die KG-Mißorientierungsmessungen mittels der *Selected-area-channelling*-Methode zeigen, daß bei 1600°C nur die KG mit den höchsten Mißorientierungswinkeln benetzt sind. Das bedeutet, daß die Temperaturen des KG-Benetzungphasenübergangs für die KG mit unterschiedlichen Energien im W-Ni-System in einem breiten Intervall liegen.

SUMMARY:

The penetration of Ni along the grain boundaries (GB's) in W polycrystals at different temperatures (1600, 1800 and 2000°C) above the eutectic temperature of the W-Ni system has been investigated. At 1600°C three different groups of GB's were found: (a) GB's wet by the Ni-rich melt; (b) GB's partially wet by the Ni-rich melt; (c) GB's not wet by the Ni-rich melt. It means that the GB wetting phase transition in the W-Ni system can be observed. The measurements with aid of *selected area channelling* show that only GB's with highest misorientation angles are wet at 1600°C. It means that the GB wetting phase transition temperatures for the GB's with different energies lie in a wide temperature interval.

INTRODUCTION

The penetration and distribution of a liquid phase on the grain boundaries (GB's) plays a very important role in liquid phase sintering of refractory metals. Complete wetting of the solid by the liquid is believed necessary for full densification during liquid phase sintering of materials containing a high volume fraction of the solid phase. The parameters of liquid phase sintering (for example, the spacing between solid particles) depend critically on the wetting angles θ in the contacts between liquid phase and particles (1,2). Liquid bridges between particles with different θ may assume different forms (2), and the spacing dependencies of the force between such particles are also very different for different θ (3-5). For low wetting angles the force F between the particles is attractive and during the sintering it presses the particles together (1). For large θ the force F is repulsive at little spacings and is attractive only at large spacings (1). In this case during the sintering an equilibrium spacing exists and at lower spacings the particles repel each other. This difference between the forces for large θ and low θ controls the process of particle rearrangement. The formation of necks with low energy GB's after particle coalescence can be seen particularly well in systems like Fe-Cu (6,7) and Ag-Cu (8). It was shown (9) that in W-Ni alloys during the initial stages of sintering the original polycrystalline W powder dissolved into single crystals due to the penetration of liquid Ni along the solid GB's. However, after long sintering periods (10,11), microstructural studies clearly indicate that some of the W single crystals move about within the liquid and subsequently contact and coalesce into a single particle. This indicates that in some temperature interval above the eutectic temperature T_e in the W-Ni system the low energy GB's are not wet and the high energy GB's are wet by liquid phase.

If the GB energy σ_{GB} is higher than $2\sigma_{SL}$ (σ_{SL} is the energy of the liquid-solid phase boundary per unit area) the GB is wet and $\theta=0$ (θ is the contact angle at the site of GB intersection with the solid-melt interface, see Fig.1). If the σ_{GB} and σ_{SL} alter differently with the temperature (Fig.1c), the so-called GB wetting phase transition at T_w can proceed (12,13). Below T_w $2\sigma_{SL} > \sigma_{GB}$ and $\theta > 0$, the GB is not wet; above T_w $2\sigma_{SL} < \sigma_{GB}$, $\theta=0$, and the GB is wet (Fig.2a). The conode in the (L+ β) two-phase area (Fig.2b) schematically shows such a

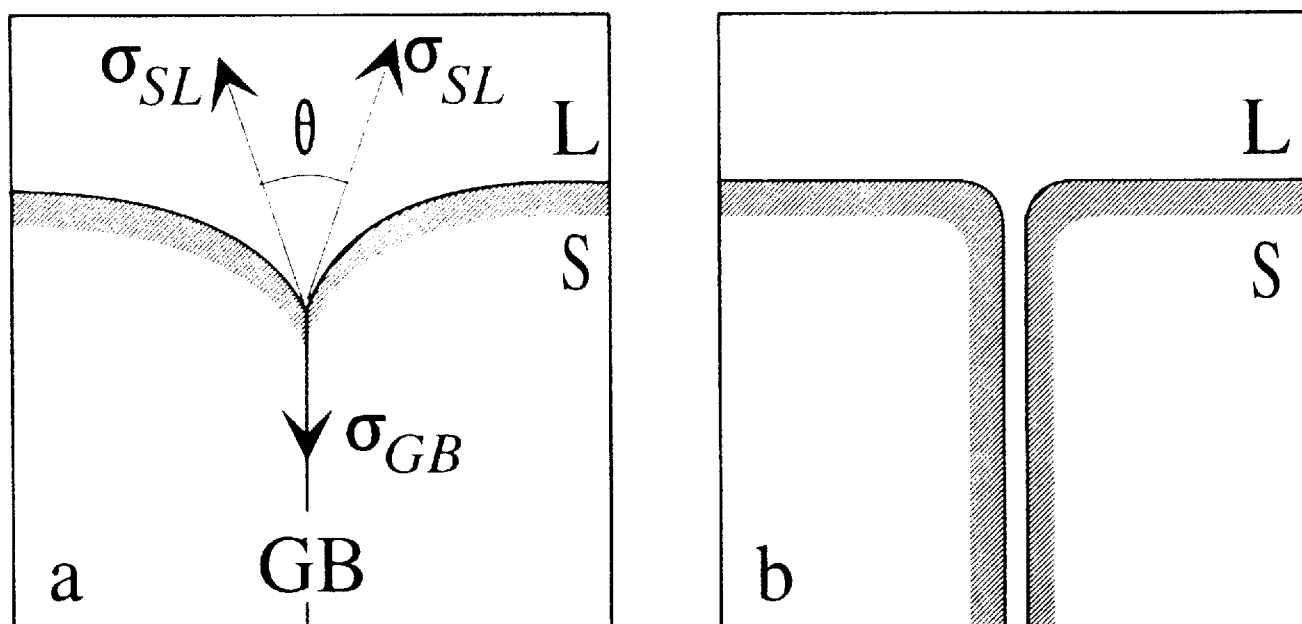


Figure 1. Bicrystal in contact with the liquid phase (L). (a) Incomplete wetting of the GB by the melt, $\theta > 0$. (b) complete wetting, $\theta = 0$.

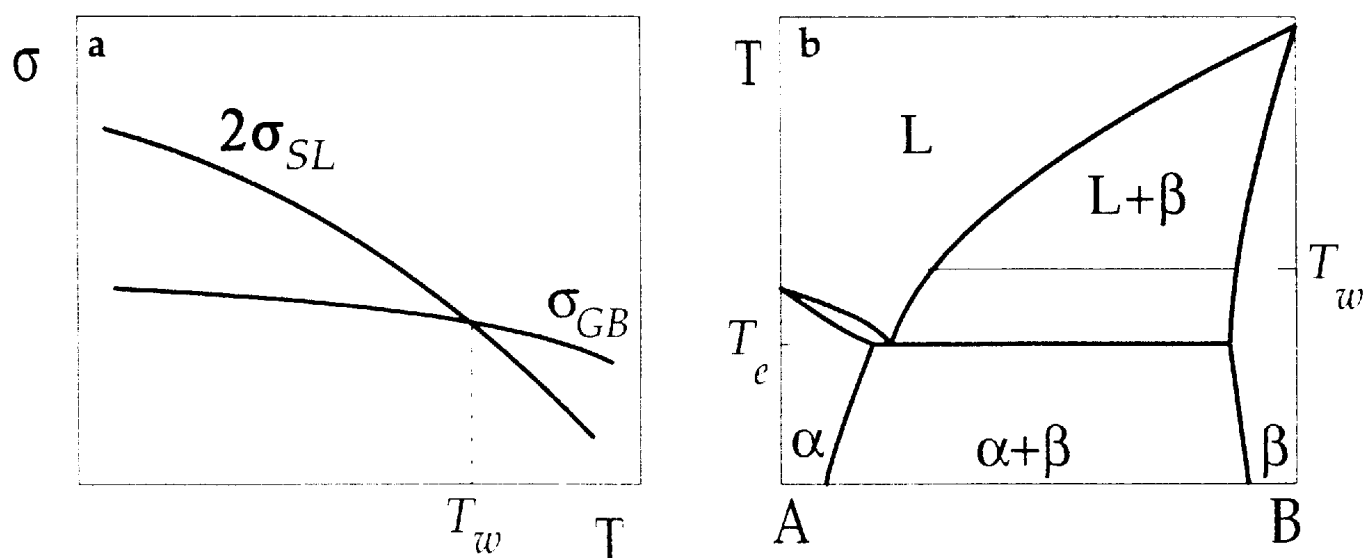


Figure 2. (a) Schematic diagram of the temperature dependencies of the energies of the grain boundaries (σ_{GB}) and the solid-liquid phase boundaries (σ_{SL}) near the GB wetting phase transition temperature T_w . (b) An idealized eutectic phase diagram for the component B with high melting temperature T_m and the component A with low T_m . The line of possible wetting GB phase transition at temperature T_w is also shown.

GB wetting phase transition. GB wetting phase transitions have been observed in the following binary and quasi-binary systems: Zn-Sn (14,15), Al-Sn (17,19), Al-Pb (17), Ag-Pb (20), (Fe-Si)-Sn (21), (Fe-Si)-Zn (21,22), Cu-Bi (23) and Cu-In(24).

Different GB's with different energies have also different wetting temperatures (24). If $\sigma_{GB1} > \sigma_{GB2}$, then $T_{w1} < T_{w2}$. For example, in the Cu-In system the wetting phase transition at the tilt GB $77^\circ \langle 110 \rangle$ in Cu occurs at $T_{w1}=930^\circ\text{C}$ and at GB $141^\circ \langle 110 \rangle$ at $T_{w2}=960^\circ\text{C}$ ($\sigma_{GB1} / \sigma_{GB2} = 1.4$) (24).

In our work it should be investigated whether it is possible to observe the GB wetting phase transition in W-Ni system and the difference between wetting temperatures for different GB's in W polycrystals. The other aim of this study was to make the first steps in investigation of the Ni-rich melt penetration along the GB's in W at different temperatures and wetting conditions.

EXPERIMENTAL

For our experiments the tablets of pure W compact (diameter 10 mm, height 5 mm) produced by Metallwerk Plansee GmbH were used. Prior to the other experiments these samples were recrystallized at 2000°C for 2 h in vacuum of 10^{-8} Pa. After recrystallization annealing the microstructure of the W specimens was investigated with aid of scanning electron microscopy (SEM), optical microscopy and selected area channelling (SAC) technique. Then a layer of Ni (about 1 mm thick) was applied on the surface of the W tablets. For this sake the axial electron beam gun was used. The scheme of making coverage is shown in Fig.3. The tablets have to be heated up to about 1000°C by electron beam, and then the drop of Ni has to be made to provide a good surface wetting. Usually this procedure takes about 30-40 s. Then the tablets were annealed at different temperatures ($1600, 1800, 2000^\circ\text{C}$; 1 h) above the eutectic temperature of the W-Ni system ($T_e=1495^\circ\text{C}$) in vacuum of 10^{-8} Pa. The cooling time was about 5 min. After the annealing the specimens were cut by the electrospark machining and the cross-section perpendicular to the Ni-covered surface was investigated with aid of optical microscopy and SAC technique. With aid of metallography the area of Ni GB penetration in the W polycrystal was investigated and the GB's wet, partially wet or not wet by Ni-rich melt were found.

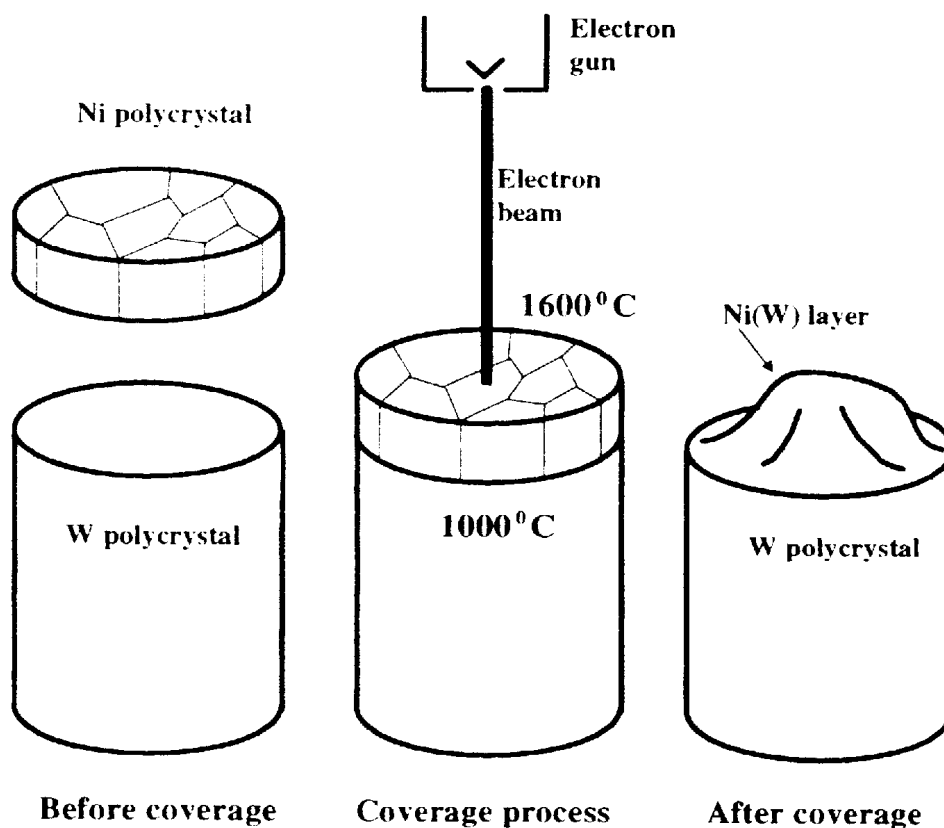


Figure 3. Method of applying a Ni layer on the surface of a W tablet

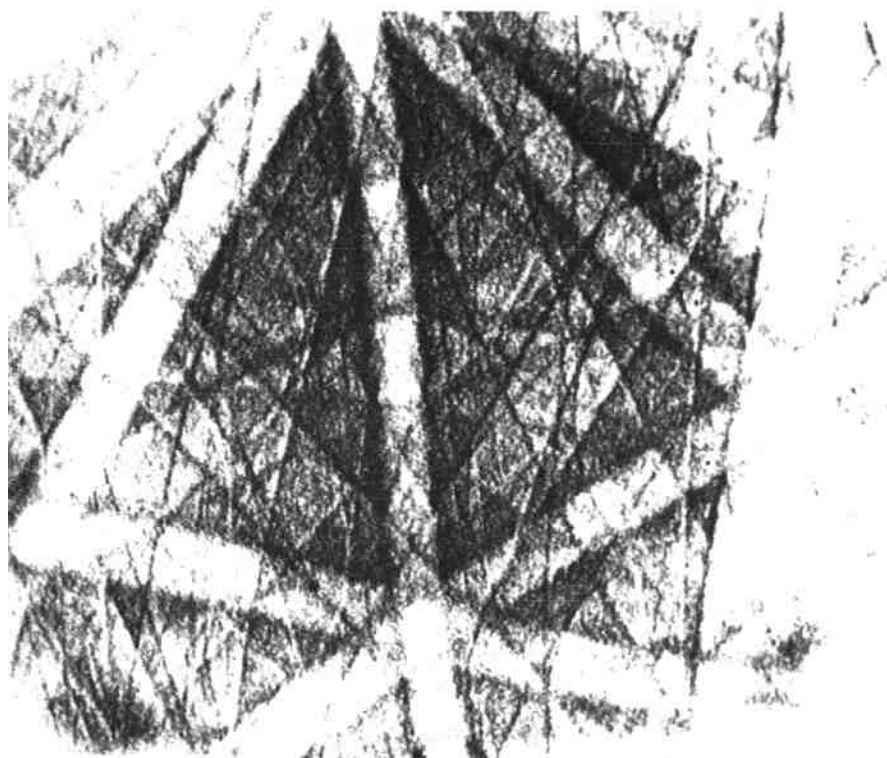


Figure 4. The typical channelling pattern for a W grain.

The SAC technique was used in order to determine the mutual misorientation of grains which form GB's wet, partially wet or not wet by the Ni-rich melt. In usual X-ray techniques the data come from a large number of grains due to the large diameter of the X-ray beam. In this case the analysis is tedious, time consuming and indirect because the actual single grain cannot be identified. Transmission electron microscopy (TEM) is the only technique which combines spatial specific diffraction information with fine microstructural details. However, there are known limitations for the application of TEM (small electron transparent region of the foil and the difficulty in relating the view area to the whole specimen). Techniques which occupy a position in between X-ray analysis and TEM are based on SEM. For example in SAC technique all grains can be seen, and misorientations assigned in the actual image (25). It means that many grains can be analysed, and the overall picture of the misorientation distribution can quickly be obtained.

The typical channelling pattern for W grain is shown in Fig.4. The orientations of the grains were measured "by hand" from a channeling pattern. A grain orientation can be obtained from a screen using only a ruler and standard map. This method was adopted as a simple computer program for routine orientation measurements. It requires the operator to identify poles in the channelling pattern. Then the screen coordinates of three points on each of two pairs of lines and of one pole are input into the computer program. These data are compared to a look-up table of rotations and interplanar spacings (bands widths) in order to index these lines and thus solve the pattern. The orientation of a grain with respect to the specimen frame may be equally described both by rotation angles and rotation axis or by proper orthogonal matrices. There are 24 geometrically different, crystallographically equivalent rotations for cubic systems. Each of these rotations describes completely the orientational position of a grain in respect to the specimen frame. The direction cosines for the zone axis and for axis perpendicular to channelling planes have been determined by a primary processing of the patterns. Those with respect to grain frame were obtained via an indexing procedure. In our work the channelling patterns and image were analysed together. In this case the orientations can be ascribed to individual grains and related to both microscopic and macroscopic features of the specimen.

RESULTS

The investigations with aid of optical metallography and SEM show that the microstructure of W polycrystals after recrystallization annealing (2000°C, 2h) contains practically equiaxed grains with size of about 30 μm (Fig.5). But some grains in this microstructure build colonies consisting of about 20-30 grains with low-angle boundaries. Between these colonies there are the "belts" of grains with high misorientations (large central part in Fig.5).

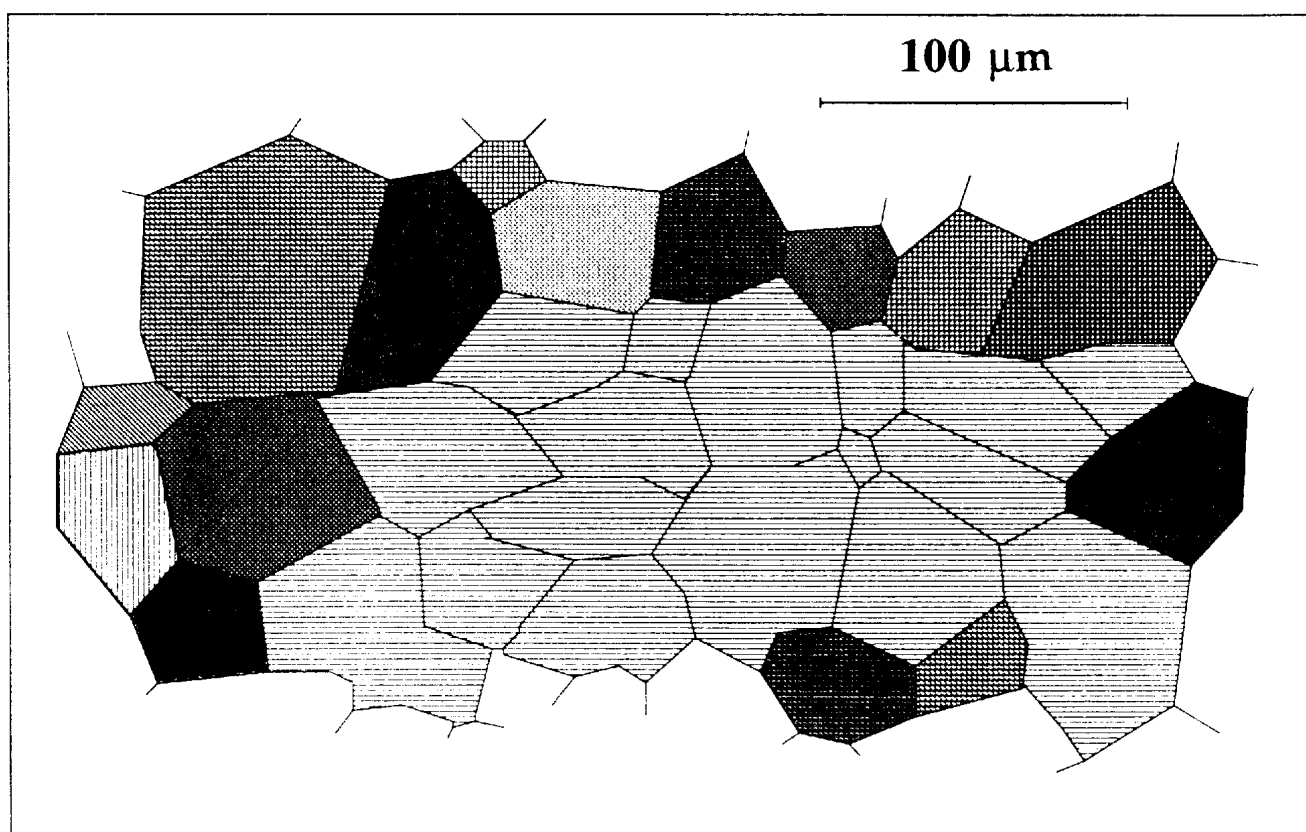


Figure 5. The microstructure of a W polycrystal after recrystallization anneal at 2000°C for 2h. Different shadings show different orientations of grains, measured with aid of selected area channelling technique.

In Fig.6 the microstructure of the W polycrystal is shown after the penetration of the Ni-rich melt from the surface at 1600°C. This temperature lies about 100°C above the eutectic temperature of the W-Ni system. The Ni-rich phase penetrated along the GB's to a depth of about 50 μm into the W polycrystal. It can be clearly seen that in the penetration layer there are three types of GB's:

- GB's which were wet with a Ni-rich melt at the annealing temperature. The Ni-rich phase formed a uniform flat thick layer on these GB's;
- GB's which were partially wet with a Ni-rich melt at the annealing temperature. The Ni-rich phase formed droplets on these GB's;
- GB's which were not wet with a Ni-rich melt at the annealing temperature. There are no visible macroscopic layers or particles of the Ni-rich phase on these GB's.

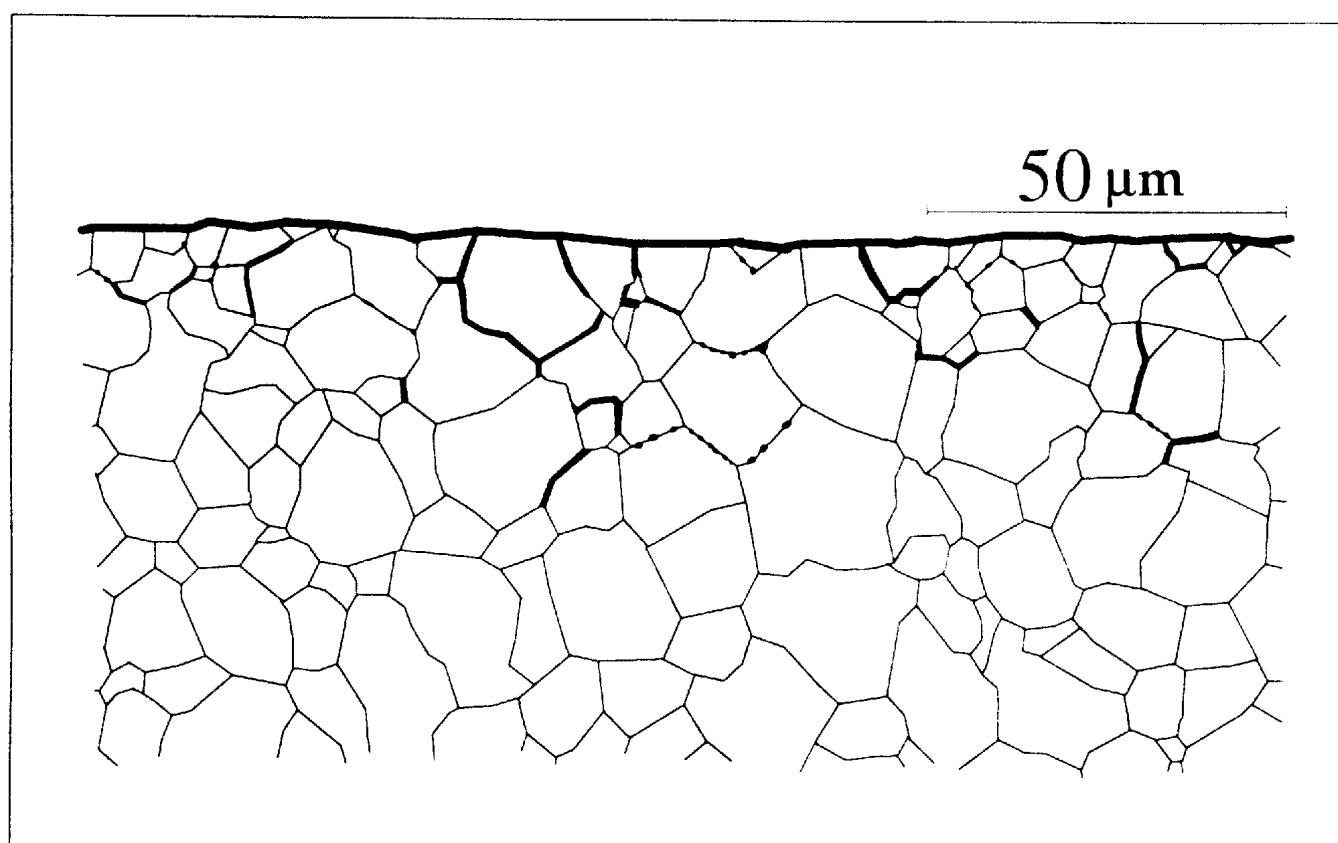


Figure 6. The microstructure of the W polycrystal after the penetration of the Ni-rich melt from the surface (top side of the figure) during the annealing at 1600°C for 1h.

The misorientation parameters of 21 GB's from all three groups of GB's in Ni penetration layer were measured with aid of SAC (Fig.7). No preferential orientations (texture) were found for the grains investigated. The misorientation angles θ for GB's which are not wet by the Ni-rich melt lie in the angular interval from 17° to 49°. The partially wet GB's (with droplets of the Ni-rich phase) have misorientation angles from 24° to 50°. The wet GB's (with a flat thick layer of the Ni-rich phase) have misorientation angles from 33° to 47°.

At higher temperatures investigated (1800 and 2000°C) Ni also penetrates along the GB's the into W polycrystal. But in these cases the penetration is more uniform: in the penetration layer there are no partially wet GB's with droplets of the Ni-rich phase.

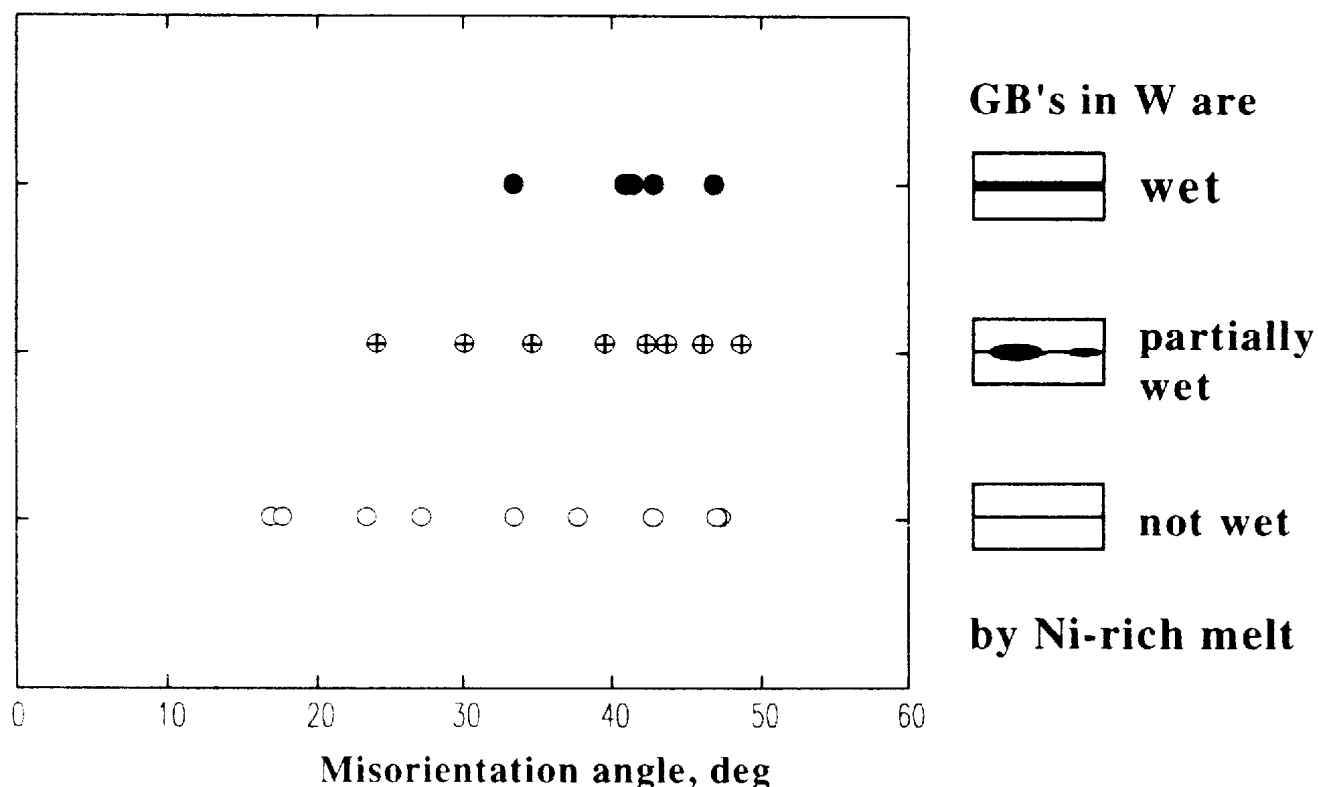


Figure 7. The misorientations of three different groups of GB's within the Ni penetration layer of W polycrystals after anneal at 1600°C for 1h. The misorientations were defined by selected area channeling SEM technique.

DISCUSSION

The comparison between the microstructures of W polycrystals after Ni penetration from the surface along the GB's at different temperatures show the following:

- at 1600°C there are three different groups of GB's within the Ni penetration layer, corresponding to wet, partially wet and not wet by the Ni-rich melt;
- at higher temperatures investigated there are only wet GB's within the Ni penetration layer.

Therefore, it can be concluded that slightly above the eutectic temperature of the W-Ni system the wetting phase transition proceeds on the W grain boundaries. Moreover, the wetting phase transition proceeds on the different grain boundaries at different temperatures. The temperature of 1600°C lies in the temperature interval, where different GB's in W becomes wet. This conclusion is based on the observation that at 1600°C some GB's are wet, and other GB's are partially wet or not wet. Therefore, the temperature interval of the GB wetting phase transition for different GB's in W(Ni) system lies between $T_e = 1495^\circ\text{C}$ and 1800°C .

In Fig.8 the scheme is shown which helps to understand the experimental misorientation distribution in the penetration layer at 1600°C (Fig.7). In Fig.8 the schematic misorientation dependence of the GB energy σ_{GB} is shown. At low misorientations θ the GB energy σ_{GB} grows with θ according to Frank formula for dislocation arrays (26). Above θ about 20° the GB energy σ_{GB} grows only slightly. At high misorientations θ there are also cusps on the $\sigma_{GB}(\theta)$ dependence near the so-called coincidence misorientations. The $\sigma_{GB}(\theta)$ dependence was not experimentally measured for GB's in W, but such data exist for other cubic metals like Al (27) and Cu (28).

On the same figure the energy $2\sigma_{SL}$ for two solid-liquid phase boundaries of GB wetting layer is shown. In the first approximation $2\sigma_{SL}$ does not depend on θ . The GB's with energy $\sigma_{GB} < 2\sigma_{SL}$ are not wet or are only partially wet. The GB's with energy $\sigma_{GB} > 2\sigma_{SL}$ are wet.

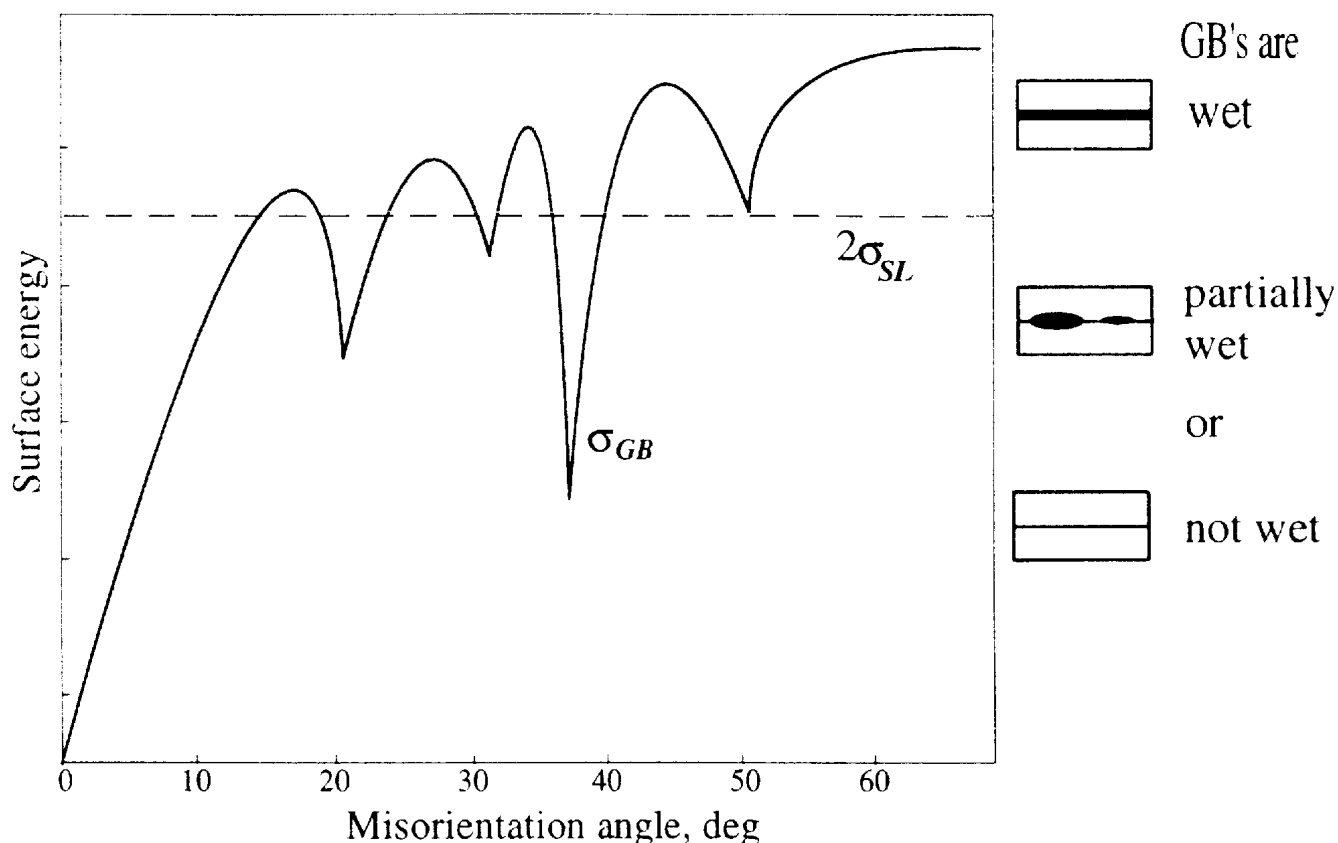


Figure 8. Scheme showing misorientation dependence of the GB energy $\sigma_{GB}(\theta)$ and the line for the energy $2\sigma_{SL}$ of two solid-liquid phase boundaries of the GB wetting layer.

This scheme clearly shows that the wet GB's must have higher misorientation angles and narrower misorientation spectrum than the GB's which are partially wet or not wet. On the other hand, the GB's which are partially wet or not wet can also have a large misorientation angle if this angle lies near the cusps on the $\sigma_{GB}(\theta)$ dependence, because near these cusps $\sigma_{GB} < 2\sigma_{SL}$.

ACKNOWLEDGEMENTS

The authors would like to thank Prof.L.S.Shvindlerman and Dr.E.Rabkin for many constructive ideas. We are also grateful to Prof.Chr.Herzig for providing the W samples and for helpful discussions.

REFERENCES

1. G.Petzow and W.J.Huppmann: *Z. Metallk.* 67 (1976) pp. 333-342.
2. W.J.Huppmann and H.Rieder: *Acta Metall.* 23 (1975) pp. 965-971.
3. R.B.Heady and J.W.Cahn: *Met. Trans.* 1 (1970) pp. 185-191.
4. J.W.Cahn and R.H.Heady: *J. Am. Ceram. Soc.* 53 (1970) pp. 406-412.
5. Yu.V.Naidich, I.A.Lavrinenko and V.N.Eremenko: *J.Powder Met.* 1 (1965) pp. 41-48.
6. S.Takayo, W.A.Kaysser and G.Petzow: *Acta Metall.* 32 (1984) pp. 115-121.
7. W.A.Kaysser, S.Takayo and G.Petzow: *Acta Metall.* 32 (1984) pp. 107-113.
8. W.A.Kaysser, S.Takayo and G.Petzow: *Z.Metallk.* 73 (1982) pp. 579-586.
9. W.J.Huppmann and H.Riegger: *Int. J. Powder Met. Technol.* 13 (1977) pp. 243-249.
10. D.N.Yoon and W.J.Huppmann: *Acta Metall.* 27 (1979) pp. 693-699.
11. D.N.Yoon and W.J.Huppmann: *Acta Metall.* 27 (1979) pp. 973-979.
12. S.Dietrich in: *Phase Transitions and Critical Phenomena*, Vol.12 (ed. by C.Domb and J.Lebowitz). Academic Press, London (1988) pp. 1-220.
13. O.I.Noskovich, E.I.Rabkin, V.N.Semenov, B.B.Straumal and L.S.Shvindlerman: *Acta Metall.* 39 (1991) 3091-3096.
14. A.Passerone, N.Eustatopoulos and P.Desré: *J. Less-Common Met.* 52 (1977) pp. 37-44.
15. A.Passerone and R.Sangiorgi: *Acta Metall.* 33 (1985) pp. 771-777.
16. B.B.Straumal, O.I.Noskovich, V.N.Semenov, L.S.Shvindlerman, W.Gust and B.Predel: *Acta Metall. Mater.* 40 (1992) pp. 795-801.
17. K.K.Ikeuye and C.S.Smith: *Trans. Am. Inst. Min. Engrs.* 185 (1949) pp. 762-770.
18. N.Eustatopoulos, L.Coudurier, J.C.Joud and P.Desré: *J. Cryst. Growth* 33 (1976) pp. 105-111.
19. J.H.Rogerson and J.C.Borland: *Trans. Am. Inst. Min. Engrs.* 227 (1963) pp. 2-8.
20. A.Passerone, R.Sangiorgi and N.Eustatopoulos: *Scripta Metall.* 16 (1982) pp. 547-552.
21. E.I.Rabkin, V.N.Semenov, L.S.Shvindlerman and B.B.Straumal: *Acta Metall. Mater.* 39 (1991) pp. 627-639.
22. L.S.Shvindlerman, W.Lojkowski, E.I.Rabkin and B.B.Straumal: *C. Phys.Coll.C1* 51 (1990) pp. 629-635.
23. H.J.Vogel and L.Ratke: *Acta Metall. Mater.* 39 (1991) pp. 641-648.

24. B.Straumal, T.Muschik, W.Gust and B.Predel: *Acta Metall. Mater.* 40 (1992) pp. 939-945.
25. V.Randle: *Microtexture determination and its applications*, The Institute of metals, London (1992) pp. 134-178.
26. W.Bollmann: *Crystal Defects and Crystalline Interfaces*, Springer Verlag, Berlin (1970) pp. 302-352.
27. G.C.Hasson and C.Goux: *Scripta Metall.* 5 (1971) 889-895.
28. H.Miura, M.Kato and T.Mori: *C.Physique* 51-C1 (1990) 263-269